ISSN: 2633-4828 Vol. 5 No.1, January, 2023

International Journal of Applied Engineering & Technology

AERODYNAMICS ANALYSIS AND EFFECT OF WIND DISTURBANCE ON CHRYSLER 300S CAR MODEL USING FLUENT- ANSYS 18IN DIFFERENCES ANGELES

Aseel Ali Hussien and Mustafa Munadil Kadhim
Mechanical Engineering Department, Collage of Engineering, Thi-Qar University, Iraq
aseelalftlawy91@gmail.com and mustafamunadil@gmail.com

Date of Submission: 06th December 2022 Revised: 25th January 2023 Accepted: 20th February 2023

ABSTRACT

These days, as the car industry becomes more competitive, vehicle aerodynamics is crucial. Because aerodynamics changes some factors, such lift and drag forces, which are important at high speeds, the vehicle's performance is impacted. Manufacturers are turning away from wind tunnel testing in favorite of computational fluid dynamics due to advancements in computer technology, which will shorten testing times and save R&D expenses. In this paper, the pressure and the velocity distributions on the surface of the vehicle's body under the influence of wind have been studied at different angles (35°, 90°, and 125°). The parameters that affect the steering system of vehicle have been studied, using the CFX ANSYS (18.2) simulation programs. The torque and the effort have been calculated on the steering system by using the mathematical equation in the MATLAB program .We found the values of torque on the pinion in the cases of the vehicle when it affected by wind in several cases where the highest value was recorded in the fourth case 26.1(N-m) when the vehicle is facing the air and at the corner 90° *where there are two entrances to the air.*

Keywords: cfd; drag; drag force,; vortex generator; Ansys; fluent;

I. INTRODUCTION

The number of cars on the road in Iraq is predicted by the country's present economic development trajectory. However, this rise would also result in a significant increase in CO2 emissions, which would have a negative impact on the environment. As a result, automakers are searching for novel approaches and creating cutting-edge technology to lower fuel use and boost vehicle economy.

drag is a significant influence in vehicle economy, which is why vehicle aerodynamics is a topic of intense study for automakers. Although wind tunnel testing was the most advanced method of assessing vehicle aerodynamics in the 20th century, numerical simulations are becoming more and more common due to recent advances in processing capacity. By analysing flow behaviour without the need to build a physical model, computational fluid dynamics (CFD) helps save time and money on research and development.[1] The magnitude of the aerodynamic forces is depending upon the velocity of the vehicle and density of the air. These two factors can affect the performance of the vehicle. At different velocity we would be get different amount of drag force and also at different density of the air we would get different amount of force. Density of the air is depending upon the ambient temperature. If the temperature is too low then the density of the air become high which causes drag and lift forces will increases. If temperature is gradually reduces so density of the air will also reduce which causes decreasing drag and lift forces. [2]

Stojanovic .N et. al (2023) .[3] Using SolidWorks software, models of the passenger car without and with a rear spoiler (types S1 and S2) are generated. Utilising the ANSYS software/Fluid Flow (CFX) module, a comprehensive analysis of these models was conducted utilising a numerical approach. The objective was to optimise the vehicle's speed while simultaneously ensuring its stability. The findings from the numerical analysis demonstrated that the longitudinal stability incensement is significantly impacted by the spoiler, particularly when operating at high velocities. The stability of the spoiler is not significantly impacted by its shape. The lift force of the vehicle with the spoiler (type S2) was 7.6 times less than that of the vehicle without the spoiler. A 12% increase in drag force was observed with the implementation of the spoiler (type S2). The impact of the rear spoiler's presence on the passenger car was examined, along with the influence of the spoiler's shape and

construction dimensions on its longitudinal stability. An integrated approach was devised, which incorporated both the design and numerical analysis of the stability of the vehicle. The efficacy of a developed approach in mitigating the adverse effects of certain factors to improve vehicle stability was demonstrated.Patel, D. et al (2018) [4] Focuses on the CFD analysis of a production vehicle CFD analyses successfully carried out on the production car. The outcomes of the simulation (drag coefficient) have been determined to be in close agreement with the officially provided values. Once the validity of the simulation become achieved, the next step became to make changes within the geometry of the original version that can positively affect performance traits (lift and drag). A diffuser was added to the rear cease of the vehicle and similarly simulations have been performed. The addition of an eight deg. Diffuser helped lessen the raise considerably (34% reduction in Cl) while handiest slightly growing the drag coefficient (0.5% growth in Cd). Increasing the diffuser angle to ten deg. after which 15 deg. led to a extra discount in lift. However, the corresponding drag penalties have been also better. The effects obtained by way of acting the consistent state analysis were then confirmed by appearing a temporary simulation, both offering a similar fee of Cd. The addition of a diffuser to the original version at an attitude of 8 tiers showed a definite improvement within the car raise traits with a negligible drag penalty. Such changes will be performed in the decided on car to enhance its handling skills at higher speeds thereby enhancing the overall safety of the car.

II. OBJECTIVE

The CFD study of a manufacturing vehicle is the main topic of this research. The availability of the car in Iraq is the first criterion for choosing. b) The vehicle drag coefficient as officially given (as a reference to confirm the correctness of the simulation findings). c) The availability of car blueprints, which are required to make a CAD model.

Given that the chosen car meets the aforementioned criteria and is well-liked in Iraq, it has been chosen. Using Solidworks 2018, the car model is examined using (Fluent Analysis Software: Ansys 18.) The objective is to accurately calculate the vehicle's drag and lift coefficient by simulating the airflow around the Chrysler 300. The next stage would be to alter the geometry of the car, which might enhance its lift and drag characteristics and boost fuel economy while also improving the vehicle's handling at cruising speeds.

III. THEORY

Computational fluid dynamics, or CFD, is a subfield of fluid mechanics that solves and analyses fluid flow problems numerically using computers. Computations are performed on computers via an iterative process in which the precision of the result increases with each iteration. The Navier-Stokes equations are the basic equations that are solved in CFD problems. The steady-state Navier-Stokes equations, which predict the velocity and pressure fields, may be solved to fully forecast the fluid's flow in the laminar domain. It is no longer feasible to assume that the flow is time-invariant once it starts to shift into turbulence. In this instance, the issue must be solved in the time domain. The flow field displays tiny eddies as the Reynolds number rises, and the oscillations' timescales are so short that solving the Navier-Stokes equations computationally becomes impractical. Given the fact that the flow field over time includes tiny, local oscillations that may be addressed in a time-averaged manner, a Reynolds Averaged Navier-Stokes formulation can be used in this flow regime.

A. RANS

The Reynolds Averaged Navier-Stokes equations (also known as RANS equations) are equations used to predict the fluid flow using a time averaged formulation. The primary concept applied is Reynolds decomposition which involves decomposing an instantaneous quantity into its time averaged and fluctuating quantities. The time averaged nature of its equations makes it an attractive choice while simulating turbulent flows. Considering certain approximations based on the knowledge of properties of turbulent flows, these equations can be used to give time averaged solutions to the Navier– Stokes equations.

B. K-epsilon Model

The k-epsilon model is one of the most commonly used turbulence models. It is a two equation model that employs two extra transport equations to represent the turbulent properties of the flow. This allows a two equation model to account for history effects like convection and diffusion of turbulent energy. This model, however, does not perform well in cases of large adverse pressure gradients.

C. Realizable k Epsilon Model

The realizable k-epsilon model addresses the well-known deficiencies of the traditional k-epsilon model by incorporating:

- A new eddy-viscosity formula involving a variable C_μ originally proposed by Reynolds.
- A new model equation for dissipation based on the dynamic equation of the mean square velocity fluctuation.

This model makes it possible to achieve good results in terms of integral values (eg. Cd) which are within 2-5% of the actual value. It is also very stable and converges quickly.

D. Non-Equilibrium Wall Function (NWF)

For high Reynolds number flows, such as in external flow around vehicles, resolving the near wall region down to the wall is not practical. To overcome this, wall functions are used. NWF takes into account the effects of local variation in the thickness of the viscous sublayer, when computing the turbulent kinetic energy budget in wall adjacent cells. Besides this, NWF is also sensitized to adverse pressure gradients which are common in flow around vehicles. Compared to traditional wall functions, NWF provide more realistic predictions of the behaviour of the turbulent boundary layers, including flow separation, and they do so without a significant increase in either CPU time or dynamic memory.

E. Aerodynamic Devices - Diffuser

The wake area behind a vehicle is a low pressure region which has a retarding effect on the vehicle. A diffuser is a modification in the vehicle geometry which helps counter this effect by gradually increasing the air pressure from the underbody towards the rear. At the beginning of the diffuser, the air accelerates due to the sudden change in the shape of the underbody and creates a low pressure point. As we move towards the rear bumper, the diffuser expands which causes the pressure to increase gradually upto ambient pressure at the rearmost of the vehicle. Thus, a diffuser has a combined effect of increasing the downforce at the vehicle rear while simultaneously reducing the low pressure wake region created behind the vehicle.

IV. PRE PROCESSING

A. Vehicle Geometry Modeling

For modeling the geometry, 3D modeling software Solidworks 2018 was used. The modeling process involved importing the vehicle Chrysler300s blueprints into Solidworks with the help of which, 3D curves were projected. These curves then acted as boundaries to generate surfaces. The final surface model was converted into a solid part (refer Figure. 1) before importing it to Ansys.

Figure 1: Top: Actual model view; Bottom: Solid works model.

B. Creating Fluid Enclosure

In order to simulate the air flow around the vehicle, a fluid volume needs to be created which will encompass the vehicle. This was done by creating an enclosure around the vehicle and subtracting the vehicle body. This enclosure acts as the air domain. To reduce the overall computational cost and time, the vehicle was considered symmetric laterally. The size of the enclosure was taken to be 3.3 car lengths each; ahead of the car, above the car and beside the car whereas 7.2 car lengths spacing was left between the car rear and the end of the enclosure as shown in Figure. 2

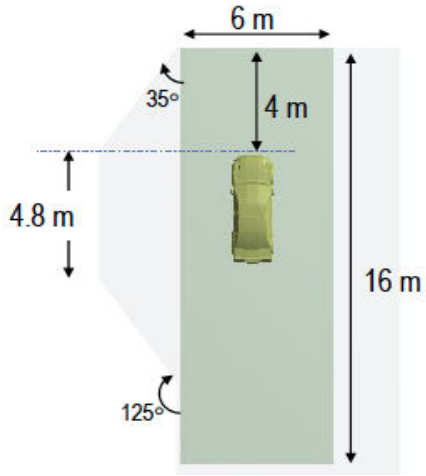

Figure 2: The computational domain (control volume).

C. Mesh Generation

While generating the mesh, sizing functions were used wherever necessary in order to obtain accurate lift/drag parameters. Two bodies of refinements were added to properly capture the flow in the region closest to the vehicle and also capture the flow in the wake. Since boundary layer separation has a significant effect on drag, five layers of inflation were added to the vehicle surface to properly resolve the boundary layer. The total number of elements obtained was 13.8 million. Figure. 2 shows the final mesh.

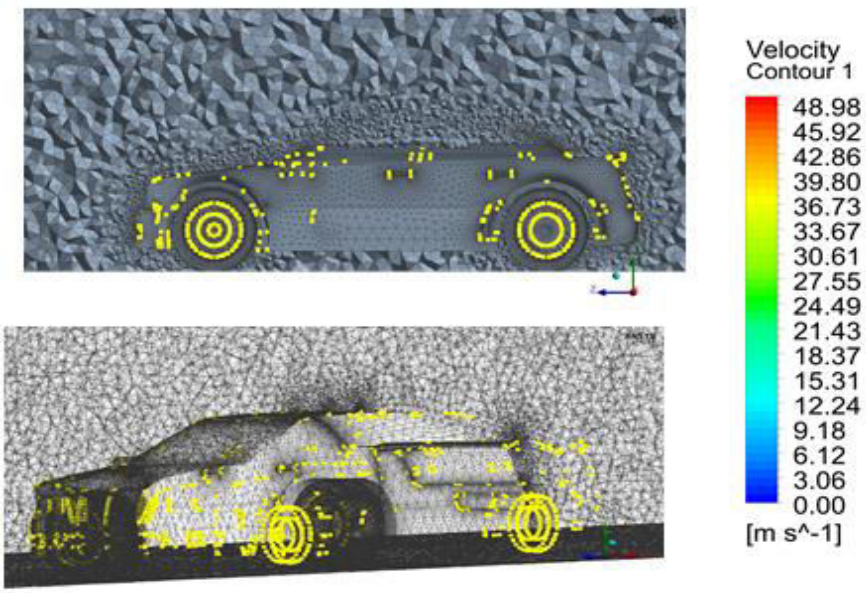

Figure 2: Mesh generated.

D. Boundary Conditions

The enclosure inlet plane was named "velocity-inlet". Air coming through the inlet was given a velocity of 120 km/h. The road and the vehicle body were both made walls. The surrounding enclosure surfaces, being imaginary surfaces, were all named symmetry planes having a „no slip" condition. The outlet was named a "pressure-outlet" with its pressure set constant and equal to atmospheric pressure.

V. SOLVER

For this analysis, a pressure based steady state solver was used. The solution methods, equations used along with the input data are listed below:

- Pressure based steady state solver.
- Realizable k- epsilon model with non-equilibrium wall functions.
- Air velocity at inlet: 150 km/h
- Reference area to determine drag and lift coefficients – Frontal Area: 1.17425 m^2.

The final solution was obtained by performing the iterations in three stages. With each progressive stage, the solver accuracy was raised by employing higher order equations. In the first stage, first order equations were used to prevent the solution from diverging. The Pseudo Transient Scheme was selected to speed up convergence. Once sufficient convergence was achieved, the equation order was raised. The iterations were carried up to the point where the change in the value of drag coefficient was found negligible.

VI. GOVERNING EQUATIONS

The condition should be considered alongside the Navier-Stokes equation

1. Steady-state and turbulent flow.

2. The fluid is inviscid (no viscous dissipation) and incompressible

3. The velocity of flow is constant and uniform.

4. The mean density and pressure are uniforms throughout the fluid.

Governing equations for steady-state, incompressible, and three-dimension

Flow the main governing equations are about conservation of mass and momentum Continuity equation:

$$\frac{\partial \rho}{\partial t} + \frac{\partial (\rho u_i)}{\partial x_i} = 0 \qquad (1)$$

Momentum equation:

$$\frac{\partial \rho u_i}{\partial t} + \frac{\partial (\rho u_i u_j)}{\partial x_j} = \frac{\partial \rho}{\partial x_i} + \frac{\partial}{\partial x_j}\left[\mu\left(\frac{\partial u_i}{\partial x_j} + \frac{\partial u_j}{\partial x_i}\right)\right] \qquad (2)$$

Where

ui, uj are velocity components.

ρ is air density.

P is air pressure.

μ is dynamic viscosity.

and t is time.

The domain has been created taking in consideration several aspects, as the flow in the domain is expected to be turbulent and approximately isothermal, the RNG K- ε turbulence model with as callable wall function treatment was used because of it slightly accurate predictions of the low separation.

Transport conditions for the RNG k-ε model is:

$$\frac{\partial}{\partial t}(\rho k) + \frac{\partial}{\partial x_i}(\rho k u_i) = \frac{\partial}{\partial x_j}\left(\alpha_{k\mu_{eff}}\frac{\partial k}{\partial x_j}\right) + G_k + G_b - \rho\varepsilon - Y_M + S_k \quad (3)$$

$$\frac{\partial}{\partial t}(\rho \varepsilon) + \frac{\partial}{\partial x_i}(\rho \varepsilon u_i) = \frac{\partial}{\partial x_j}\left(\alpha_\varepsilon \mu_{eff}\frac{\partial \varepsilon}{\partial x_j}\right) + G_{1\varepsilon}\frac{\varepsilon}{k}(G_k + C_{3\varepsilon}G_b) - C_{2\varepsilon}\rho\frac{\varepsilon^2}{K} - R_\varepsilon + S_\varepsilon \quad (4)$$

G_k represents the generation of turbulence kinetic energy.

G_b is the generation of turbulence kinetic energy.

Y_M represents the contribution of the fluctuating dilatation in compressible turbulence to the overall dissipation rate.

The quantities α_k and α_ε are the inverse effective Prandtl numbers for k and ε .

μ_{eff} effective viscosity.

C1ε, C2ε, and C3ε are constants.

S_k and S_ε are user-defined source terms[5].

And using the standard k–ϵ model in solid work program, that tackle two separate transport equations and that they are the foremost wide used in industrial applications as a result of it provides economy, robustness and reasonable accuracy. the primary major assumption of this model is that the turbulent viscosity μt is isotropic. The second major assumptions that the dissipation and production terms given within the k equation are approximately equal regionally [6].Two transport equations, one for the turbulent kinetic energy k is defined as the variance of the fluctuation in velocity, and an additional one for the rate of dissipation of turbulent K.E. are solved . ϵ represents the rate at that velocity fluctuation is dissipated by the action of viscosity on the tiniest eddies. the standard k–ϵ model uses the subsequent transport equations for k;

$$\rho u_j \frac{\partial k}{\partial x_i} = \frac{\partial \epsilon}{\partial x_j}((\mu + \frac{\mu_t}{\sigma\epsilon})\frac{\partial \epsilon}{\partial x_j}) + 2\mu_t S_{ij} . S_{ij} - \rho \epsilon \quad \text{.....(5)}$$

And ϵ;

$$\rho u_j \frac{\partial \epsilon}{\partial x_j} = \frac{\partial \epsilon}{\partial x_j}((\mu + \frac{\mu_t}{\sigma\epsilon})\frac{\partial \epsilon}{\partial x_j}) + C_{1\epsilon}\frac{\epsilon}{K}\mu_t S_{ij} . S_{ij} - C_{2\epsilon}\rho\frac{\epsilon^2}{K} \quad \text{.....(6)}$$

where σk and $\sigma\epsilon$ are the Prandtl numbers connecting the diffusivities of k and ϵ to the eddy viscosity μt, the strain rate tensor can be writ in terms of velocity by.

$$S_{ij} = \frac{1}{2}\left(\frac{\partial u_j}{\partial x_i} + \frac{\partial u_i}{\partial x_i}\right) \text{.....(7)}$$

The two equations above in words mean:

Transport of k or ϵ by convection = Transport of k or ϵ by diffusion

+Rate of production of k or ϵ-Rate of destruction of k or ϵ

It is noticeable that the transport equations include five adjustable constants;

σk, $\sigma\epsilon$, $C\mu$,$C1\epsilon$ and $C2\epsilon$. The values for these constants have been obtained by comprehensive data fitting to the standard k–ε model for a wide range of turbulent flows. These values are follows σk=1.00, $\sigma\epsilon$=1.30, $C\mu$=0.09, $C1\epsilon$=1.44 and $C2\epsilon$=1.92 [7].

VII. ANSYS RESULT

A. Pressure Distribution

This analysis was achieved by using the ANSYS 18.2 package. Figure4 demonstrates the contour of pressure distribution effect on the surface of the vehicle with various flow angles are(180º, 35º, 90o and 125º) and wind velocity are (120km/hr.) with steady-state, in viscid fluid and turbulent flow. The boundary conditions, all outer zones pressure are set to atmospheric pressure. It has been shown There is a higher pressure concentration on the car in the front section. The airflow will slow down when it approaches the front area of the vehicle and will result in the air accumulated into a smaller space. Once the air stagnates at the frontal area of the car, it will flow to lower pressure area such as the head and roof, sides and bottom of the car. When the air flows over the vehicle head, the pressure decreasing. However, when it reaches the windscreen, the pressure increases. When the higher pressure air in front of the windshield travel over the windshield, it accelerates, causing the decrease of the pressure. This lower pressure lately produces a lift-force on the car roof as the air passes over it.

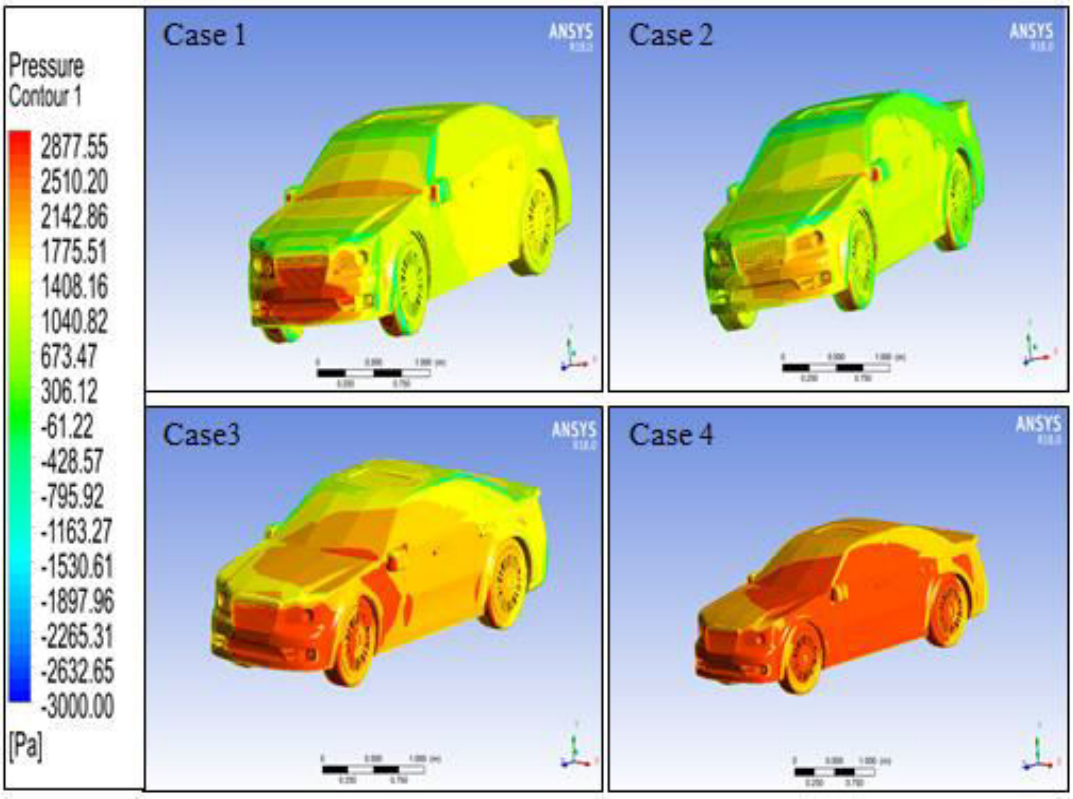

Figure 4: contour map of pressure distribution on the car

B. Velocity distribution

From the velocity distribution in figure 5 it can be observed that the velocity magnitude contours around Chrysler body along with the whole domain. it's obvious that rounded edges at the front car surface accelerate the airflow, but that airflow gets obstructed by car rear. The maximum velocity magnitude recreated the symmetry plane is79m / s which are at the area of the vehicle case_02. Also, as the car moving at a constant speed of 120km / hr. the blue region in the contour plot shows the lowest airflow velocity of the system. The lowest airflow velocity can be found there are of the vehicle It can be seen that the air velocity is decreasing as it approaches the front section of the car (blue region). The air velocity increases away from the car front to the car slide roof. The red region indicates the highest air flow velocity and can be spotted at the front side (slide roof) of the car and the backside of the car roof.

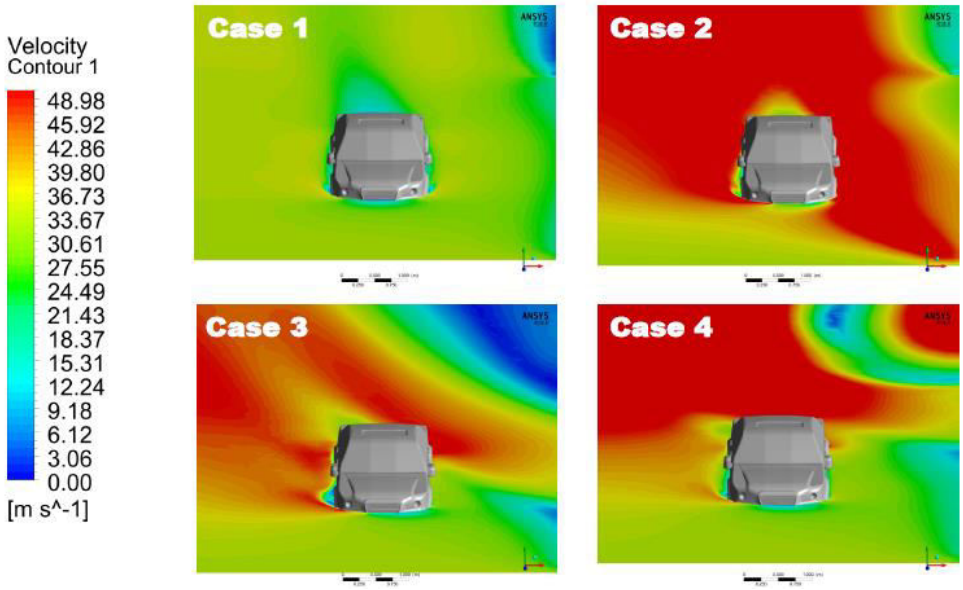

Figure 5: contour represents the velocity(m/sec) distribution

C. Turbulent Kinetic Energy

The turbulence intensity contours for front view of the vehicle were shown in figure6 there are two areas around the car body where high turbulence can be spotted which are at the front wheel area and at the rear of the vehicle. However, the result is less accurate since this study does not includes the rotating wheel in the analysis. The maximum of the turbulence intensities of the vehicle is 21.4Jfound at the rear of the vehicle.

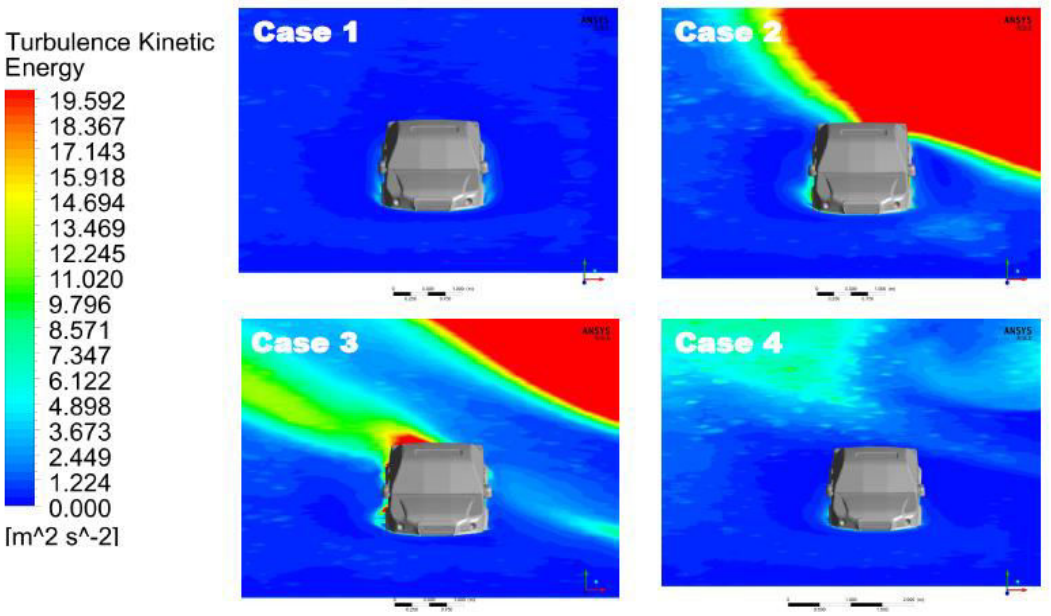

Figure 6: turbulent kinetic energy

D. Forces on Tires

Case 01 figure 7 represents the value of the forces affecting on the tires of the vehicle in case of movement When the vehicle is facing the air and has only one entrance to the air.

Case_01	Fx	Fy	Fz
Tire 1	15.9574 [N]	9.40039 [N]	-12.499 [N]
Tire 2	-17.7806 [N]	10.2166 [N]	-14.1326 [N]
Tire 3	3.90328 [N]	2.06691 [N]	-10.3814 [N]
Tire 4	-0.50921 [N]	-1.55325 [N]	-6.65254 [N]

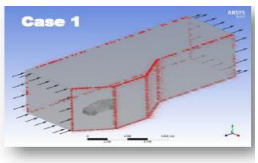

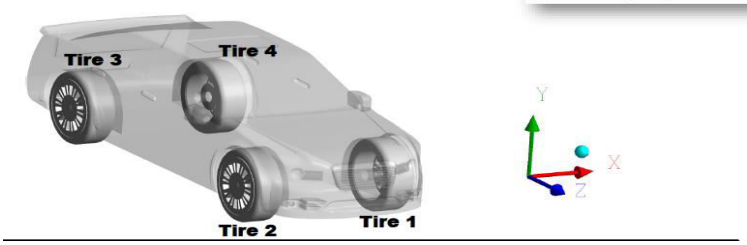

Figure 7: Case 01

Case 02 figure 8 Represents the value of the forces affecting on the tires of the vehicle in case of movement When the vehicle is facing the air and at the corner 35° where there are two entrances to the air.

Case_02	Fx	Fy	Fz
Tire 1	-20.8496 [N]	-47.6744 [N]	-62.6848 [N]
Tire 2	-86.7408 [N]	43.5148 [N]	-133.294 [N]
Tire 3	-28.1899 [N]	-26.6027 [N]	-66.6878 [N]
Tire 4	-24.7789 [N]	26.7160 [N]	-102.221 [N]

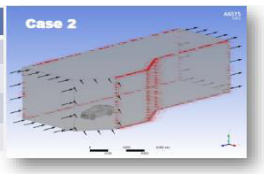

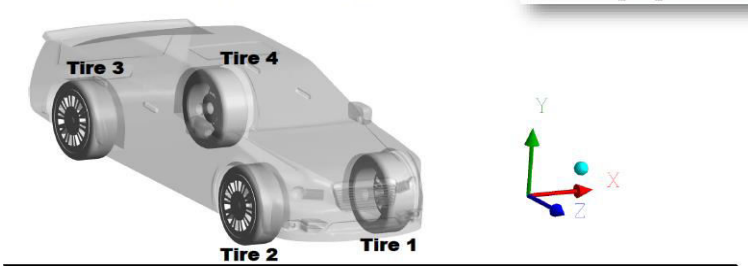

Figure 8: Case 02

Case 03figure 9 Represents the value of the forces affecting on the tires of the vehicle in case of movement When the vehicle is facing the air and at the corner 90° where there are two entrances to the air.

Case_03	Fx	Fy	Fz
Tire 1	-83.6359 [N]	-61.928 [N]	-60.4074 [N]
Tire 2	-116.774 [N]	61.0677 [N]	-92.4337 [N]
Tire 3	-72.2214 [N]	-4.63731 [N]	-69.1321 [N]
Tire 4	-49.6488 [N]	-43.2188 [N]	-83.8408 [N]

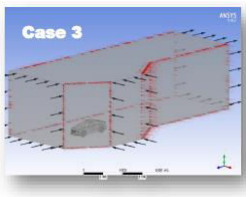

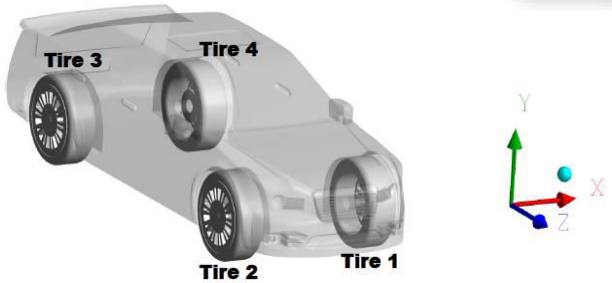

Figure 9: Case 03

Case 04figure 10 represent the value of the forces affecting on the tires of the vehicle in case of movement When the vehicle is facing the air and at the corner 90° where there are two entrances to the air

Case_04	Fx	Fy	Fz
Tire 1	-151.304 [N]	-104.6 [N]	-15.7905 [N]
Tire 2	82.6845 [N]	-69.4994 [N]	-44.7146 [N]
Tire 3	-25.224 [N]	-93.0323 [N]	-27.3901 [N]
Tire 4	-74.3133 [N]	-127.938 [N]	-83.1779 [N]

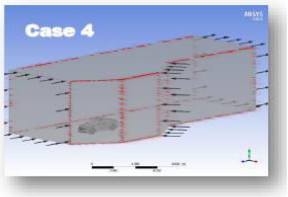

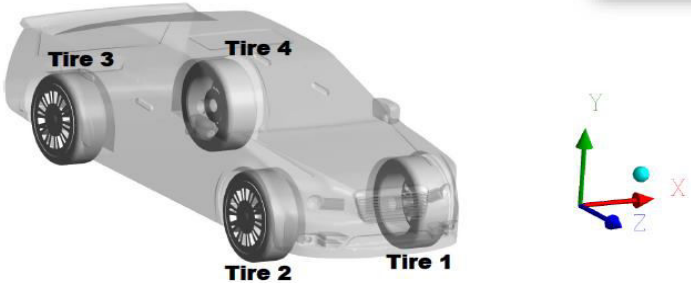

Figure 10: Case 04

VIII. RESULTS AND DISCUSSION

The results show the torque of steering wheel when the passenger car is moving at speed 120 km/hr, dynamic friction coefficient is 0.3 [8], vehicle, the stationary torque is137.2 N-m and the steering effort is = 342.9N The tires used for the vehicle are dry tires and coefficient of friction between tires and rolled gravel ground is 0.8[9] where the studying are done for passenger vehicle as Chrysler 300s .The working forces are calculated by Ansys CFX software for cases as :

Case 01: One entrance and air facing the car

Case 02: Two inlets (front one and wall with 35 degree slip angle)

Case 03: Two inlets (front one and wall with 90 degree slip angle).

Case 04: Two inlets (front one and wall with 125 degree slip angle

Table (1) torque and steering wheel effort

No.	Case	Torque (N.m)	Steering Effort (N)
1	Case 01	102.5	256.4
2	Case 02	103	258
3	Case 03	102.8	257.2
4	Case 04	104.76	261.9

In this paper the impact of the wind on the vehicle in several angles and its impact with its surrounding vehicle and drag force have been numerically studied. From the results it can be conclude the following:

1. The maximum air flow velocities recorded are in case 02when the wind faced the car and with 35 degree slip angle located around the car section.
2. The maximum pressure distribution recorded in case 03when the wind faced the car and 90 degree slip angle located around the car section.
3. The least value of the effect of vortices on the drag force in the third case when the SUV vehicle is front of the passenger car.
4. The highest value drag when the passenger car in front of the SUV vehicle.
5. Wind affects the steering wheel effort and its highest value when the wind faced the car and at 125 degrees slip angle.

Torque on Pinion

The results show the torque on pinion when the passenger car is moving at speed 120 km / hr. , dynamic friction coefficient is 0.3 [10], vehicle dimension as shown in table (1) .with effect by wind in several angles, as shown in Table (2), and the stationary torque is64.35N- m The tires used for the vehicle are dry tires and coefficient of friction between tires and rolled gravel ground is 0.8 [11] where the studying is done for passenger vehicle as Chrysler 300s. Car dimensions were listed in section (3.9.4). seven cases were discussed. The working forces are calculated by Ansys CFX software for cases as

Case 01: One entrance and air facing the car

Case 02: Two inlets (front one and wall with 35 degree slip angle)

Case 03: Two inlets (front one and wall with 90 degree slip angle).

Case 04: Two inlets (front one and wall with 125 degree slip angle

Table (2) torque on pinion

No.	Case	Torque with wind(N-m)	Torque without wind(N-m)
1	Case 01	25.187773	64.35
2	Case 02	25.2724935	
3	Case 03	25.2643898	
4	Case 04	26.1	

This table shows the values of torque on the pinion in the cases of the vehicle when it affected by wind in several cases where the highest value was recorded in the fourth case and that is because the working force with the influence of winds were the highest values and that due to the vortices formed behind the vehicle in fig. 11. and also note that the torque on the pinion in the state of the vehicle is fixed is higher than the torque in the case of wind, this torque is the added strength on the torque of assisted motor, so according to equation $T_m = \frac{N_1 K_t}{R_a}\left(e_m - K_b N_1 \theta_{sc}\right)$ ....8 .(motor input voltage) must be the largest value in order to overcome the torque of the assisted motor.

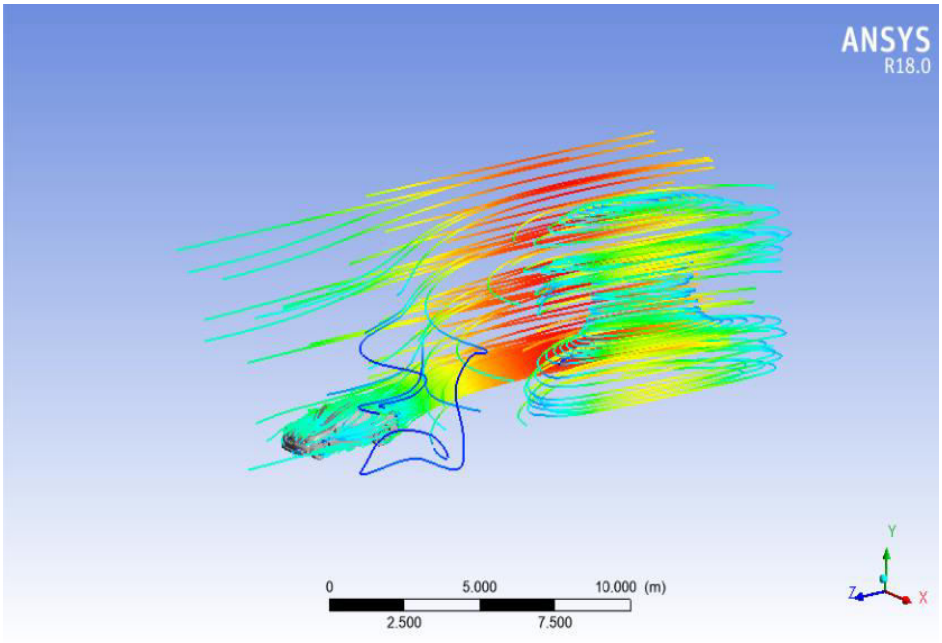

Figure 11: vortices formed behind the vehicle

IX. SIMULATION RESULTS

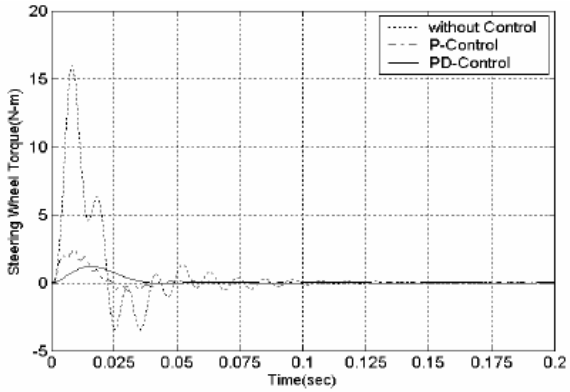

Figure 12: Impulse response of steering wheel torque.

Figure 12 For the system with proportion management, drivers are felt the high frequency oscillation once road wheel endures an impact wind . the issues in proportion control will be eliminated by using proportion-plus-derivative management. we tend to create a choice appropriate proportion gain (Kp=20000) to realize desired steering assistance level and derivative gain (Kd=300) to achieve required damping Impulse response of proportion-plus-derivative control in time domain is shown in Fig(12(solid line) and comparison with without control (dotted line) and proportion management (dash dotted line), the response is far improved, peak amplitude is lower and high frequency oscillation no longer

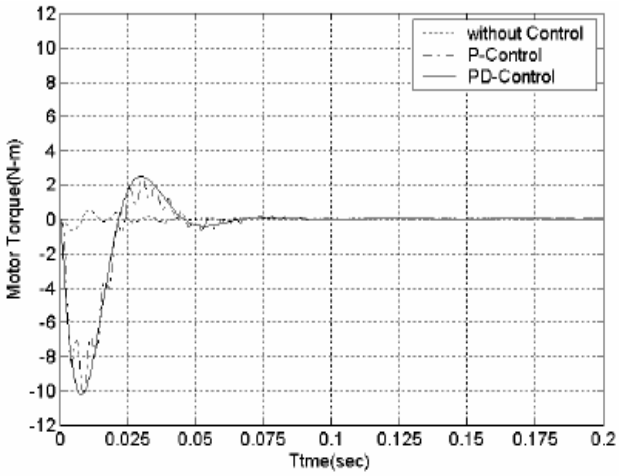

Figure 13 Assisted motor torque at steering column.

Figure 13shows assisted motor torque with relevance steering column at every control theme. within the case of without control, motor back-electromotive force act sort of a viscous damping, therefore there seems bit of damping effects in motor torque. In proportion control and proportion-plus-derivative control, motor assist force to steering column through gear-box. In proportion-plus-derivative control motor torque shows swish curve whereas proportion control shows fluctuation.

X. CONCLUSIONS

In this thesis the impact of the wind on the vehicle in several angles and its impact with its surrounding vehicle and drag force have been numerically studied. From the results it was conclude the following:

1. The maximum air flow velocities recorded are in case 02when the wind faced the car and with 35 degree slip angle located around the car section.

2. The maximum pressure distribution recorded in case 03when the wind faced the car and 90 degree slip angle located around the car section.
3. Wind effects on the vehicles and its highest value when the wind faced the car and at 125 degrees slip angle.
4. The fourth case recorded the highest reactions on tires with 125 degree slip angle. the values of torque on the pinion in the cases of the vehicle when it affected by wind in several cases where the highest value was recorded in the fourth case and that is because the working force with the influence of winds were the highest values

REFERENCES

[1] Parab, A., Sakarwala, A., Paste, B., Patil, V., & Mangrulkar, A. (2014). Aerodynamic analysis of a car model using Fluent-Ansys 14.5. International Journal on Recent Technologies in Mechanical and Electrical Engineering, 1(4), 7-13.

[2] Shrivastava, A., kumar singh , D. Mohan Mishra, P.(2018), AERODYNAMIC ANALYSIS OF THE VEHICLE USING THE SOLIDWORK FLOW SIMULATION, International Journal of Recent Trends in Engineering & Research (IJRTER),V(4),PP. 2455-1457

[3] Stojanovic, N., Abdullah, O. I., Grujic, I., Glisovic, J., & Belhocine, A. (2023). The influence of spoiler on the aerodynamic performances and longitudinal stability of the passenger car under high speed condition. *Journal of Visualization*, *26*(1), 97-112.

[4] Patel, D., Jangid, J., Devani, Y., Goswami, S., & Vachhani, M. (2018). CFD Analysis on Aerodynamics of an Automobile Body.

[5] Thet Mon Soe , San Yu Khaing, Comparison of Turbulence Models for Computational Fluid Dynamics Simulation of Wind Flow on Cluster of Buildings in Mandalay International Journal of Scientific and Research Publications, Vol. 7, n. 8, 2017.

[6] Thomas Vyzikas, " Application of numerical models and codes", MERiFIC, 1st ed., February (2014).

[7] H K Versteeg and W Malalasekera, "An Introduction to Computational Fluid Dynamics, The Finite Volume Method", Prentice Hall, ISBN: 978-0-13-127498-3, 2nd Ed., (2007).

[8] https://whyps.com/understanding-hydraulic-power-steering-system

[9] Minh, V. T. (2012, October). Vehicle steering dynamic calculation and simulation. In Proceedings of the 23rd International DAAAM Symposium on Intelligent Manufacturing and Automation, Zadar, Croatia (pp. 24-27).

[10] G. & Nilsson, H. (2006). Vehicle Stability Control for Roadside Departure Incidents by Steering Wheel Torque Superposition, Master's Thesis, department of Applied Mechanics & Signals and Systems, Chalmers Uinversity of Technology, Göteborg, Sweden

[11] Li, Z., Shi, S., & Zhang, C. (2018). Active Return Control Strategy of Electric Power Steering System Based on Disturbance Observer. Journal of Engineering Science & Technology Review, 11(3).